Editorial

# Intracranial aneurysms: looking beyond size in neuroimaging: the role of anatomical factors and haemodynamics

**Dylan Pau Roi[1], Jens-Dominik Mueller[2], Kyriakos Lobotesis[1], Cathal McCague[3], Sabrina Memarian[1], Faraan Khan[4], Kshitij Mankad[5]**

[1]Imperial College NHS Healthcare Trust, London, UK; [2]Queen Mary's University of London, London, UK; [3]John Radcliffe Hospital, Oxford, UK; [4]St George's Hospital, London, UK; [5]Great Ormond Street Hospital, London, UK

*Correspondence to:* Dr. Dylan Pau Roi. Imperial College NHS Healthcare Trust, London, UK. Email: Dylan.roi@nhs.net.

Submitted Feb 19, 2019. Accepted for publication Mar 26, 2019.
doi: 10.21037/qims.2019.03.19
**View this article at:** http://dx.doi.org/10.21037/qims.2019.03.19

## Introduction

Some cerebral aneurysms are diagnosed incidentally; others may present symptoms due to the pressure exerted on surrounding structures, and local processes such as inflammation. They are, however, frequently diagnosed after a subarachnoid hemorrhage (SAH), following aneurysm rupture. SAH carries a high mortality and morbidity, and incidence of 6–8/100,000 (1). Lifetime cost-per-year of survival following SAH is 3× as high as elective surgery or endovascular treatment of patients with an unruptured aneurysm (UA) (2). Thus, estimated risk of rupture is a key factor in deciding how to treat UA.

A meta-analysis conducted by Rinkel *et al.* (3) found cerebral aneurysm prevalence of 2.3% in adults with no risk factor for SAH. In a subgroup of nine prospective angiographic studies of patients with known risk factors for SAH (n=3,751) the prevalence increased to 6%. Prevalence of aneurysms also increased with age, peaking in the age group of 60–79 years.

Managing aneurysms neurosurgically or endovascularly carries risk in itself; hence, it is desirable to quantify rupture risk in UA. Currently, treatment decisions are not based on recognized criteria or parameters but rather an individual appreciation of anatomical features like size and location. These provide an incomplete assessment of rupture risk.

Haemodynamically driven mechanisms involving the arterial wall have been linked to aneurysm initiation and subsequent growth in both *in vivo* and modeled environments. Clearly, the evolution of an aneurysm is governed by interaction between blood flow and vessel wall, however current modalities do not offer non-invasive insight into wall properties (4).

## Aneurysm characteristics

The PHASE scoring system (5) was based on a meta-analysis of the largest cohort available currently. Patient factors such as ethnicity, age, previous history of SAH, or history of hypertension are considered alongside aneurysmal factors including size and location to stratify patients according to rupture risk. Higher scores suggest higher aneurysm rupture risk. However, this tool requires further validation and the treatment of a significant proportion of patients in the follow-up time may have resulted in a selection bias.

### *Size*

A meta-analysis of 6,556 aneurysms in all intracerebral locations (average age 55.6, 70% female) (6) demonstrated an increased rupture risk with increasing size. Aneurysms of 5 to 10 mm in diameter were 2.3 times more likely to rupture (95% CI: 1.0–5.2) compared to smaller ones. Risk increased to 11.9 for aneurysms greater than 15 mm (95% CI: 5.5–25.8). The UCAS cohort (n=6,697) showed a similar trend, with increased risk of rupture as the maximal aneurysm diameter increased.

However, of the patients presenting with SAH (n=245), 86% had aneurysms smaller than 10 mm (7). Anterior

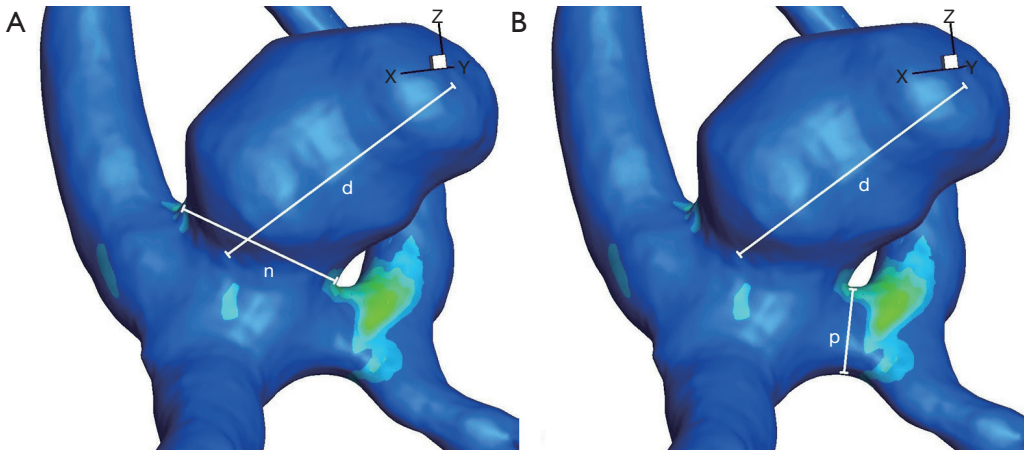


**Figure 1** Three dimensional computational model of an anterior communicating artery aneurysm. (A) Aspect ratio (AR) as maximal aneurysm diameter (d) over neck diameter (n); (B) size ratio (SR) as maximal aneurysm diameter (d) over parent vessel diameter (p).

communicating (ACom) aneurysms were the most common (29.0%), of which 94.4% were smaller than 10 mm, suggesting that small aneurysms are not as benign as previously thought.

### *Location*

Aneurysm site correlates with rupture risk (8). A study of 854 ruptured aneurysms (RA) presenting with SAH (an additional 180 UA were found in the same patients), found the most common sites were: ACom 31.3%, middle cerebral artery (MCA) 24.1%, and internal carotid artery (ICA) 22.8%. The two most frequent sites of RA of less than 5mm were 48.7% ACom and MCA 11.4%.

In the UCAS cohort, MCA aneurysms (36.2%) were twice as common as ICA (18.6%), ACom (15.5%) or ICA/posterior communicating (PCom) (15.5%) aneurysms (9). However, small ACom and PCom aneurysms (<7 mm) were more likely to rupture than in others in the follow-up period.

### *Aneurysm morphology*

The UCAS cohort (9) featured 1,266 aneurysms (18.9% of aneurysms) with daughter sacs, conferring a rupture hazard ratio of 1.63 (P=0.02). Similar data in patients with two or more aneurysms at time of presentation suggested that irregular shape was associated with rupture (adjusted odds ratio =3.0, 95% CI: 1.0-8.8; n=124, totalling 302 aneurysms) (10).

### *Aspect ratio (AR)*

AR is the ratio of the maximum dimension of the dome of the aneurysm to the width of its neck (*Figure 1A*). In a study of 201 aneurysms (11), high AR correlated with risk of rupture in all locations. The authors observe that the area of neck is the limiting factor to blood inflow to the aneurysm.

A larger study of 532 patients (127 unruptured, 405 ruptured) (12) echoes these findings. Mean size difference between both groups was not significant. The mean AR of 1.8 for unruptured lesions was well below the 3.4 for those that ruptured.

### *Size ratio (SR)*

SR is the ratio of the maximal diameter of the aneurysm to that of the parent vessel (*Figure 1B*). Forty successive patients (UA n=24, RA n=16) with similar risk factor profiles, genders and parent vessel diameter were studied prospectively (13). SR was greater in the RA group [RA 4.08 (SD 0.54) *vs.* UA 2.57 (SD 0.24)] and was the only predictive factor when subjected to logistic regression analysis. In a larger cohort of patients presenting with SAH (n=854) (14.6% had more than one aneurysm, adding 180 UAs to study), diameter and SR were both significantly higher in the RA group (8) (P<0.001 for both parameters). However, in a subgroup analysis of aneurysms less than 5 mm (n=236 RA, n=138 UA), SR was significantly greater in the RA group [RA 3.2 (SD 1.2), UA 2.2 (SD 1.2), P<0.01]. These findings suggest greater risk of rupture with aneurysms arising from small arteries.

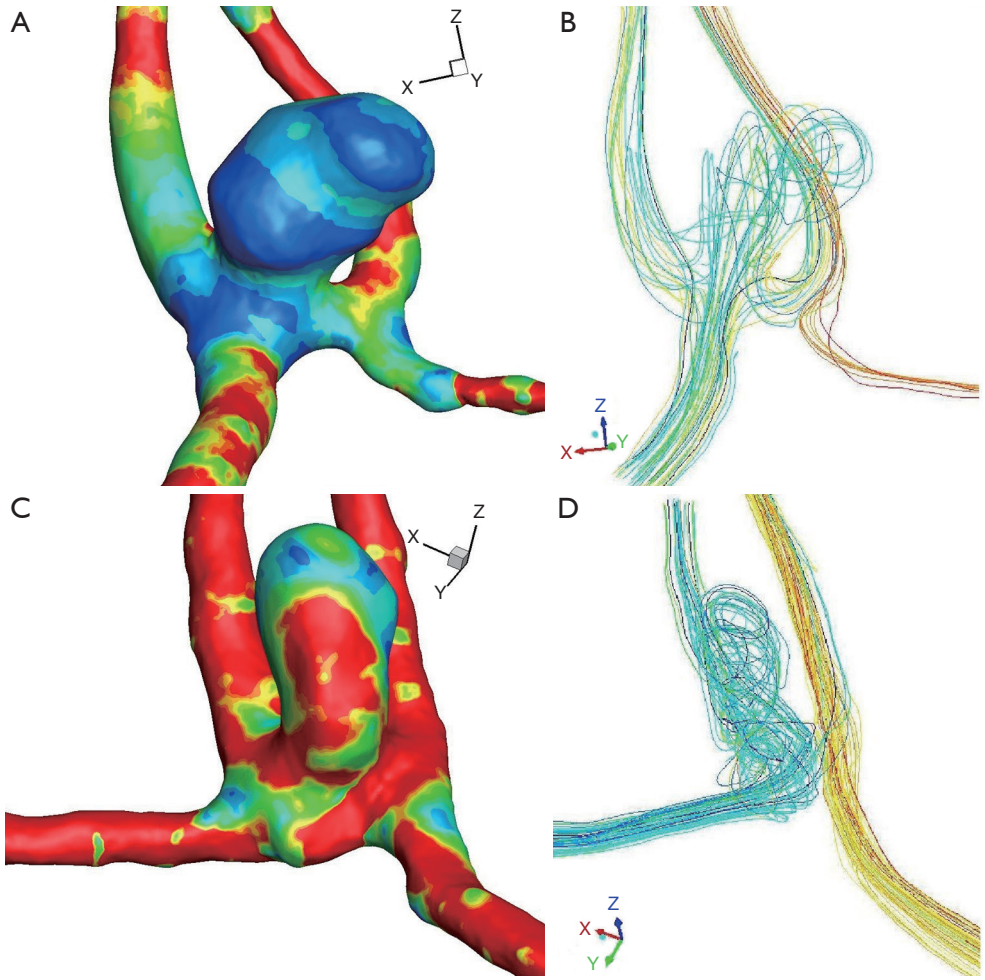


**Figure 2** Wall shear stress plots (left, A and C) and corresponding flow lines (right, B and D) for two different anterior communicating artery aneurysms [top (A and B) and bottom (C and D) respectively] with characteristics described as follows. (A) Hypoplastic right A1; (B) corresponding flow lines with exclusive filling from dominant left A1; (C) small angle (approximately 90°) of left A1–A2 segment; (D) corresponding flow lines with aneurysm filling exclusively from left A1.

### *Parent vessel geometry*

The configuration of the aneurysm and its feeding vessel(s) is significant. ACom aneurysms were related to the presence of a dominant A1 (see *Figure 2A,B*) (57% *vs.* 14% in control group, P=0.01), or a hypoplastic contralateral A1 [24% *vs.* 6% in control group, P=0.01], which may have led to increased haemodynamic forces at the ACom (14) (n=51, ACom aneurysms *vs.* 50 matched controls). Seventy-eight percent of aneurysms were filling exclusively from a single A1. These findings were reproduced by two further studies (15,16).

Kasuya *et al.* (15) looked at the angles between A1 and A2 segments of the ACA as a possible cause of aneurysm formation in 23 patients with ACom aneurysms and normoplastic A1s matched to 21 controls. Aneurysm formation was linked to smaller A1–A2 angles (mean 103° *vs.* 142.2° in the control group) as smaller angles project the impingement point onto the ACom rather than the A2 segment, thus inflicting higher haemodynamic stresses (*Figure 2C,D*).

Following observations of the previous groups, Lazzaro and colleagues (17) studied the role of circle of Willis (CoW) anatomical variants (with non-symmetrical blood supply) in aneurysm rupture of 113 patients (75% ruptured) treated for ACom or PCom aneurysms. CoW variants around the ACom complex, defined as hypoplasia or absence of the A1 segment contralateral to the aneurysm, were seen in 46.9%

 

of patients suffering rupture compared with 29.6% in the unruptured group.

## Computational fluid dynamics (CFD)

Though often used in industry as an analysis tool, CFD can also be used as a modelling tool in medical applications where *in vivo* testing is not possible. CFD numerically approximates the solution to the Navier-Stokes equations which govern fluid motion.

### *Sensitivity and limitations of a CFD approach*

Although CFD sensitivity has been validated (18), this was on the basis of multiple approximations. Watton *et al.* (19) mentions the computationally expensive yet important role of cyclic stretch in blood vessels on accurate simulations. Vessel wall boundary is simulated as "no-slip" whereas glycocalyx coated endothelial cells (ECs) allow flow even at the wall (20). The lack of patient specific inflow velocity measurements is a problem in most models (21). Mesh size also effects the solution; however, mesh convergence studies can be used to ensure appropriate mesh quality. Castro *et al.* (22) describe the challenge of accurately modelling ACom aneurysms especially around the neck as the spatial resolution of current modalities is often too low. Correlating haemodynamics and aneurysm rupture has limitations, as geometry of the aneurysm is the only information available from imaging (histological wall composition is not accounted for in simulation) (23). Finally, the impact on simulation of any change in aneurysm morphology post rupture is not factored in.

### *Flow characteristics and rupture risk*

Cebral *et al.* (24) performed CFD on 210 aneurysms (127 ruptured, 60%), establishing a classification based on the following four haemodynamic patterns: flow complexity, flow stability, inflow concentration and flow impingement zone compared to area of aneurysm. RA were 4.7× more likely to have complex flow (P<0.0001), 2.7× more likely to have unstable flow (P=0.0018), 4.0× more likely to have a concentrated inflow (P<0.0001), and 3.0× more likely to have a small impingement area (below 50% of aneurysm area) (P=0.0006). In addition, complex and unstable flow was seen more frequently in ACom aneurysms. In a more recent study (n=119 aneurysms, 38 RA and 81 UA), most RAs (61%) had complex flow patterns with multiple vortices, in contrast to most UAs (75%) with simple flow patterns and a single vortex (25).

Castro *et al.* (26) analysed 26 patients (18 ruptured, 69%) with ACom aneurysms. They too noted that aneurysms with small impingement area were more likely to rupture (83% *vs.* 63%). Seventy-seven percent of aneurysms with asymmetric A1 inflow had ruptured compared to 25% of those with symmetric inflow. The complicated flow patterns, with the more prevalent asymmetrical A1 flows, may explain the higher ACom rupture rates. They observe that the greater the asymmetry in flow the higher the rupture rate. This has also been observed clinically, as described above.

## Wall shear stress (WSS) and aneurysm growth

### *Aneurysm initiation mechanisms*

To study haemodynamics before and after aneurysm formation in three ACom aneurysms (27), a mesh was created with and without an aneurysm (idealized). All patients had a dominant A1. All reconstructions before aneurysm growth show areas of high WSS where the aneurysm later developed relative to areas of lower WSS surrounding this region.

This approach was reproduced in the ICA (n=3) to investigate the correlation between known aneurysm location and a new index characterising WSS variation (28). WSS in the artery before and after aneurysm formation was low compared to the rest of the vessel. At the locus of ICA aneurysm formation, the authors observed a "local spatial minimum" WSS, indicating a zone of stagnation. This highlights that high WSS initiation mechanism suggested by Castro *et al.* (27) is not the only mechanism to consider. In three patients imaged pre- and post-aneurysm formation, increased WSS with high spatial WSS gradient were found at all sites where aneurysms later developed (29). Aneurysm bleb formation is also associated with areas of high wall-shear-stress within the aneurysm dome (30).

### *Mechanisms of growth*

Imaging follow-up over time can be used to better understand haemodynamics seen in growing aneurysms. Three distinct studies (31-33) involving ten patients with aneurysms in different locations found that low WSS was seen in areas of growth, and when imaged more than twice

 

the trend of reducing WSS over time continued (32). In the largest cohort (n=7) imaged with magnetic resonance angiography (MRA), the mean aneurysm sac displacement of 0.19 mm (SD 0.34, range: 0.26–1.96 mm) was smaller than the size of one voxel, raising questions about the sensitivity of these measures (31). However, areas where displacement exceeded 0.3 mm had a significantly lower mean WSS than those that had grown lessor amounts [0.76 Pa (SD 1.51) *vs.* 2.55 Pa (SD 3.65) respectively, P≤0.001].

Using idealised models, different diameters and neck width were used to create a range of ARs (1.8, 2.5, and 3.0) (34). WSS was high at the neck area where the flow impinged, but low in the dome for all dimensions. WSS and pressure both decreased with increasing diameter, correlating well with findings of other research groups in this section. With increasing AR, WSS decreased whilst pressure increased in the aneurysm, leading the authors to infer that "*low WSS and high pressure ... may play important roles in the fragile change of the aneurysm and its final rupture*".

Two aneurysms picked to closely match average characteristics of 40 aneurysms studied in a previous paper (35) were used to study the link between SR and WSS: one basilar tip (terminal artery), and one sidewall artery aneurysm. With constant aneurysm morphology, different SRs were modelled by enlarging either the vessel or the aneurysm to achieve ratios ranging from 1 to 3.5. Findings reproduced in both cases showed that with increasing SR flow became more complex, with multiple vortices. Low SR led to a stable single vortex flow in both aneurysms. The area of low WSS (less than 0.5 Pa) increased dramatically when SR increased beyond 2.

### *Cohort WSS studies*

Takao *et al.* (36) studied 50 internal carotid/PCom aneurysms and 50 MCA aneurysms followed-up (13 ruptured during the study time, 6 in PComs and 7 in MCA vasculature). Low WSS was associated with rupture but only statistically significant in ICA PCom bifurcation aneurysms. Small numbers of RA may explain lack of statistical significance in MCA cohort. In a larger cohort of exclusively MCA aneurysms (n=106, 43 RA, 63 UA), low WSS was independently associated with rupture status after multivariate analysis (mean WSS RA =7.19 Pa *vs.* UA =9.55 Pa, P=0.0001) (37). In RAs, WSS values were lower within the aneurysm than in the parent vessels, whereas in UAs, they were comparable (n=119 aneurysms, 38 ruptured and 81 unruptured) (25). RAs had lower WSS magnitudes and larger areas of low WSS than UAs.

Using MRA and MR 4D fluid dynamics data, aneurysms in all common locations were analyzed (139 UA and 13 RA) (38). Low WSS and high flow variability were seen in similar percentages between RA and UA (92% and 89% respectively). However, WSS magnitude overall was significantly lower in ruptured cohort [RA 0.49 (SD=0.12) *vs.* UA 0.64 (SD 0.15), P<0.01]. Though only a small number of RAs were studied, aneurysm specific boundary conditions could be applied with this imaging modality.

## Hemodynamics and the pathology of aneurysm development

Meng *et al.* (39) hypothesized that aneurysmal development is a three-way interactive process involving aneurysmal geometry, flow conditions and pathobiology, all of which are driven by haemodynamics. Although geometry and haemodynamics are considered mutually causal, the evolution of cerebral aneurysm begins with the interplay of geometry and flow conditions, the driving forces of aneurysm remodelling and growth through pathobiology. This dynamic process leads to geometric aneurysmal growth changes, resulting in either stability or a haemodynamic stress much greater than wall strength leading to rupture.

Elevated WSS may trigger the aneurysm initiation process with changes including: increased leukocyte adhesion, damage to ECs, increased matrix metalloprotease activity (40). High WSS triggered a predominantly mural cell mediated pathway leading to thin walled hypocellular lesions, described as type I aneurysms (39).

Cerebral vascular beds are exposed to higher WSS than elsewhere in the body. The CoW has many bifurcations with zones exposed to high WSS under normal physiological flow (41), making high WSS a likely aneurysm initiation mechanism.

A uniform shear stress field aligns ECs in the direction of flow, while low WSS and changing flow direction cause loss of EC orientation (42). Low WSS also switches EC phenotype from atheroprotective to atherogenic increasing EC turnover rate. Low WSS also causes stagnation, accumulation of red blood cells and adhesion of platelets (43). This is closely followed by infiltration of white blood cells and deposition of fibrin (44). Hypoxia may also be an aggravating factor in zones of stagnation (41). Meng *et al.* (39) suggested an inflammatory cell-mediated

 

pathway induced by low WSS and high oscillatory shear index led to thick-walled atherosclerotic lesions, or type II aneurysms.

A review of 71 aneurysms retrieved post-surgery showed RAs often featured a destroyed EC layer, replaced by blood cells and fibrin (45). No smooth muscle cells (SMCs) or type IV collagen were present, and inflammatory cells such as macrophages and leukocytes had colonized the area. In most cases of severe EC disruption, vessel wall integrity was compromised.

Ruptured lesions tend to have decellularized aneurysm wall with matrix degeneration and high levels of inflammation (46). The authors hypothesize that inflammation is a result of wall degeneration rather than its cause, with inflammation triggered by a dysfunctional EC layer, due to abnormal haemodynamic stresses. Macrophages and vascular SMCs (VSMCs) are the main inflammatory components driving the pathogenesis of intracranial aneurysms (IA), with recent studies linking macrophage infiltration with increased aneurysm progression (47).

SMC apoptosis is seen in aneurysm wall (48), along with elevated concentrations of serum elastase (49) and matrix metalloproteases responsible for intracellular matrix degeneration (50). Decreased numbers of ECs, degeneration of the internal elastic lamina and thinning of the media were also reported by Stehbens (51). On a genetic level Wei *et al.* (52) discussed the regulatory role of differentially expressed genes (DEGs) on cell proliferation and apoptosis of vascular SMCs, which in turn may contribute to the progression of IA. Hormones have also been implicated: Wáng *et al.* demonstrated the protective role oestrogen plays on EC layers through the local delivery of 17β-estradiol and subsequent improved endothelial function (53).

Other epidemiological risk factors include age and smoking; smoking appears to affect every step in the cascade of events leading to SAH from hemodynamic stress and endothelial dysfunction to aneurysm wall weakening and rupture (54). Interestingly, aneurysmal SAH has a bimodal age distribution pattern (55). Jung observed that advancing age and vascular risk factors are likely to account for the older age peak whereas the intrinsic wall defects contribute to the younger-age peak.

## Conclusions

The link between anatomy and haemodynamics is key to understanding the natural history of an aneurysm and the related risk of rupture. Anatomically, though simple measurements like diameter are useful, neck size (AR) and parent vessel diameter (SR) provide more accurate measures of risk, especially in small aneurysms. From a haemodynamic perspective RA tend to have low WSS, but additional factors are also present. Not all aneurysms followed up increase in size (56). Thus, analysing aneurysm growth exclusively in the context of WSS is unlikely to reliably predict rupture risk. Currently, no single haemodynamic stress mechanism can account for aneurysm formation; rather it is likely that different factors affect different stages of growth. Research to-date suggests the solution will be though combining haemodynamic and anatomical factors to improve this risk-stratification process.

In conclusion, CFD analysis may not be the sole solution to aneurysmal risk-assessment, but may uncover geometrical and morphological characteristics affecting the rupture risk of an aneurysm. Indeed, if the relationship between pathological processes, WSS and aneurysm sac geometry is elucidated, the simple metric analysis mentioned above could be used more for decision making, negating the need for lengthy CFD analyses in everyday clinical practice.

## Acknowledgements

None.

## Footnote

*Conflicts of Interest:* The authors have no conflicts of interest to declare.

## References

1. Hacein-Bey L, Provenzale JM. Current imaging assessment and treatment of intracranial aneurysms. AJR Am J Roentgenol 2011;196:32-44.
2. King JT, Ratcheson RA. Cost and outcomes analysis. Neurosurg Clin N Am 1998;9:629-40.
3. Rinkel GJ, Djibuti M, Algra A, van Gijn J. Prevalence and Risk of Rupture of Intracranial Aneurysms: A Systematic Review. Stroke 1998;29:251-6.
4. Sanchez M, Ecker O, Ambard D, Jourdan F, Nicoud F, Mendez S, Lejeune JP, Thines L, Dufour H, Brunel H, Machi P, Lobotesis K, Bonafe A, Costalat V. Intracranial Aneurysmal Pulsatility as a New Individual Criterion for

 

Rupture Risk Evaluation: Biomechanical and Numeric Approach (IRRAs Project). AJNR Am J Neuroradiol 2014;35:1765-71.
5. Greving JP, Wermer MJ, Brown RD Jr, Morita A, Juvela S, Yonekura M, Ishibashi T, Torner JC, Nakayama T, Rinkel GJ, Algra A. Development of the PHASES score for prediction of risk of rupture of intracranial aneurysms: a pooled analysis of six prospective cohort studies. Lancet Neurol 2014;13:59-66.
6. Wermer MJ, van der Schaaf IC, Algra A, Rinkel GJ. Risk of rupture of unruptured intracranial aneurysms in relation to patient and aneurysm characteristics: an updated meta-analysis. Stroke 2007;38:1404-10.
7. Forget TR, Benitez R, Veznedaroglu E, Sharan A, Mitchell W, Silva M, Rosenwasser RH. A review of size and location of ruptured intracranial aneurysms. Neurosurgery 2001;49:1322-5; discussion 1325-6.
8. Kashiwazaki D, Kuroda S. Size Ratio Can Highly Predict Rupture Risk in Intracranial Small (<5 mm) Aneurysms. Stroke 2013;44:2169-73.
9. UCAS Japan Investigators, Morita A, Kirino T, Hashi K, Aoki N, Fukuhara S, Hashimoto N, Nakayama T, Sakai M, Teramoto A, Tominari S, Yoshimoto T. The natural course of unruptured cerebral aneurysms in a Japanese cohort. N Engl J Med 2012;366:2474-82.
10. Backes D, Vergouwen MD, Velthuis BK, van der Schaaf IC, Bor AS, Algra A, Rinkel GJ. Difference in aneurysm characteristics between ruptured and unruptured aneurysms in patients with multiple intracranial aneurysms. Stroke 2014;45:1299-303.
11. Ujiie H, Tamano Y, Sasaki K, Hori T. Is the aspect ratio a reliable index for predicting the rupture of a saccular aneurysm? Neurosurgery 2001;48:495-502; discussion 502-3.
12. Weir B, Amidei C, Kongable G, Findlay JM, Kassell NF, Kelly J, Dai L, Karrison TG. The aspect ratio (dome/neck) of ruptured and unruptured aneurysms. J Neurosurg 2003;99:447-51.
13. Rahman M, Smietana J, Hauck E, Hoh B, Hopkins N, Siddiqui A, Levy EI, Meng H, Mocco J. Size ratio correlates with intracranial aneurysm rupture status: A prospective study. Stroke 2010;41:916-20.
14. Charbel FT, Seyfried D, Mehta B, Dujovny M, Ausman JI. Dominant A1: angiographic and clinical correlations with anterior communicating artery aneurysms. Neurol Res 1991;13:253-6.
15. Kasuya H, Shimizu T, Nakaya K, Sasahara A, Hori T, Takakura K. Angles between A1 and A2 segments of the anterior cerebral artery visualized by three-dimensional computed tomographic angiography and association of anterior communicating artery aneurysms. Neurosurgery 1999;45:89-93; discussion 93-4.
16. González-Llanos F, Pascual JM, Roda JM. Anatomic and hemodynamic study of anterior communicating artery complex. Neurocirugia (Astur) 2002;13:285-98.
17. Lazzaro MA, Ouyang B, Chen M. The role of circle of Willis anomalies in cerebral aneurysm rupture. J Neurointerv Surg 2012;4:22-6.
18. Ford MD, Nikolov HN, Milner JS, Lownie SP, Demont EM, Kalata W, Loth F, Holdsworth DW, Steinman DA. PIV-Measured Versus CFD-Predicted Flow Dynamics in Anatomically Realistic Cerebral Aneurysm Models. J Biomech Eng 2008;130:021015.
19. Watton PN, Selimovic A, Raberger NB, Huang P, Holzapfel GA, Ventikos Y. Modelling evolution and the evolving mechanical environment of saccular cerebral aneurysms. Biomech Model Mechanobiol 2011;10:109-32.
20. Savery MD, Damiano ER. The endothelial glycocalyx is hydrodynamically relevant in arterioles throughout the cardiac cycle. Biophys J 2008;95:1439-47.
21. Karmonik C, Yen C, Grossman RG, Klucznik R, Benndorf G. Intra-aneurysmal flow patterns and wall shear stresses calculated with computational flow dynamics in an anterior communicating artery aneurysm depend on knowledge of patient-specific inflow rates. Acta Neurochir (Wien) 2009;151:479-85.
22. Castro MA, Putman CM, Cebral JR. Patient-specific computational fluid dynamics modeling of anterior communicating artery aneurysms: a study of the sensitivity of intra-aneurysmal flow patterns to flow conditions in the carotid arteries. AJNR Am J Neuroradiol 2006;27:2061-8.
23. Robertson AM, Watton PN. Computational fluid dynamics in aneurysm research: critical reflections, future directions. AJNR Am J Neuroradiol 2012;33:992-5.
24. Cebral JR, Mut F, Weir J, Putman CM. Association of hemodynamic characteristics and cerebral aneurysm rupture. Am J Neuroradiol 2011;32:264-70.
25. Xiang J, Natarajan SK, Tremmel M, Ma D, Mocco J, Hopkins LN, Siddiqui AH, Levy EI, Meng H. Hemodynamic-morphologic discriminants for intracranial aneurysm rupture. Stroke 2011;42:144-52.
26. Castro MA, Putman CM, Sheridan MJ, Cebral JR. Hemodynamic patterns of anterior communicating artery aneurysms: a possible association with rupture. AJNR Am

 

J Neuroradiol 2009;30:297-302.
27. Castro MA, Putman CM, Cebral JR. Computational analysis of anterior communicating artery aneurysm shear stress before and after aneurysm formation. J Phys: Conf Ser 2011;332:012001.
28. Mantha A, Karmonik C, Benndorf G, Strother C, Metcalfe R. Hemodynamics in a cerebral artery before and after the formation of an aneurysm. AJNR Am J Neuroradiol 2006;27:1113-8.
29. Kulcsár Z, Ugron Á, Marosfoi M, Berentei Z, Paál G, Szikora I. Hemodynamics of cerebral aneurysm initiation: The role of wall shear stress and spatial wall shear stress gradient. Am J Neuroradiol 2011;32:587-94.
30. Russell JH, Kelson N, Barry M, Pearcy M, Fletcher DF, Winter CD. Computational fluid dynamic analysis of intracranial aneurysmal bleb formation. Neurosurgery 2013;73:1061-8; discussion 1068-9.
31. Boussel L, Rayz V, McCulloch C, Martin A, Acevedo-Bolton G, Lawton M, Higashida R, Smith WS, Young WL, Saloner D. Aneurysm growth occurs at region of low wall shear stress: patient-specific correlation of hemodynamics and growth in a longitudinal study. Stroke 2008;39:2997-3002.
32. Sugiyama S, Meng H, Funamoto K, Inoue T, Fujimura M, Nakayama T, Omodaka S, Shimizu H, Takahashi A, Tominaga T. Hemodynamic analysis of growing intracranial aneurysms arising from a posterior inferior cerebellar artery. World Neurosurg 2012;78:462-8.
33. Tanoue T, Tateshima S, Villablanca JP, Viñuela F, Tanishita K. Wall shear stress distribution inside growing cerebral aneurysm. AJNR Am J Neuroradiol 2011;32:1732-7.
34. Wang Q, Wang WZ, Fei ZM, Liu YZ, Cao ZM. Simulation of Blood Flow in Intracranial ICA-PComA Aneurysm Via Computational Fluid Dynamics Modeling. J Hydrodyn Ser B 2009;21:583-90.
35. Tremmel M, Dhar S, Levy EI, Mocco J, Meng H. Influence of Intracranial Aneurysm-To-Parent Vessel Size Ratio on Hemodynamics and Implication for Rupture. Neurosurgery 2009;64:622-30; discussion 630-1.
36. Takao H, Murayama Y, Otsuka S, Qian Y, Mohamed A, Masuda S, Yamamoto M, Abe T. Hemodynamic differences between unruptured and ruptured intracranial aneurysms during observation. Stroke 2012;43:1436-9.
37. Miura Y, Ishida F, Umeda Y, Tanemura H, Suzuki H, Matsushima S, Shimosaka S, Taki W. Low wall shear stress is independently associated with the rupture status of middle cerebral artery aneurysms. Stroke 2013;44:519-21.
38. Kawaguchi T, Nishimura S, Kanamori M, Takazawa H, Omodaka S, Sato K, Maeda N, Yokoyama Y, Midorikawa H, Sasaki T, Nishijima M. Distinctive flow pattern of wall shear stress and oscillatory shear index: similarity and dissimilarity in ruptured and unruptured cerebral aneurysm blebs. J Neurosurg 2012;117:774-80.
39. Meng H, Tutino VM, Xiang J, Siddiqui A. High WSS or Low WSS? Complex interactions of hemodynamics with intracranial aneurysm initiation, growth, and rupture: Toward a unifying hypothesis. Am J Neuroradiol 2014;35:1254-62.
40. Dolan JM, Kolega J, Meng H. High Wall Shear Stress and Spatial Gradients in Vascular Pathology: A Review. Ann Biomed Eng 2013;41:1411-27.
41. Penn DL, Komotar RJ, Sander Connolly E. Hemodynamic mechanisms underlying cerebral aneurysm pathogenesis. J Clin Neurosci 2011;18:1435-8.
42. Ford MD, Alperin N, Lee SH, Holdsworth DW, Steinman DA. Characterization of volumetric flow rate waveforms in the normal internal carotid and vertebral arteries. Physiol Meas 2005;26:477-88.
43. Sforza DM, Putman CM, Cebral JR. Hemodynamics of Cerebral Aneurysms. Annu Rev Fluid Mech 2009;41:91-107.
44. Crompton MR. Mechanism of growth and rupture in cerebral berry aneurysms. Br Med J 1966;1:1138-42.
45. Kataoka K, Taneda M, Asai T, Kinoshita A, Ito M, Kuroda R. Structural fragility and inflammatory response of ruptured cerebral aneurysms. A comparative study between ruptured and unruptured cerebral aneurysms. Stroke 1999;30:1396-401.
46. Frösen J, Tulamo R, Paetau A, Laaksamo E, Korja M, Laakso A, Niemelä M, Hernesniemi J. Saccular intracranial aneurysm: pathology and mechanisms. Acta Neuropathol 2012;123:773-86.
47. Chalouhi N, Atallah E, Jabbour P, Patel PD, Starke RM, Hasan D. Aspirin for the Prevention of Intracranial Aneurysm Rupture. Neurosurgery 2017;64:114-8.
48. Hara A, Yoshimi N, Mori H. Evidence for apoptosis in human intracranial aneurysms. Neurol Res 1998;20:127-30.
49. Chyatte D, Lewis I. Gelatinase Activity and the Occurrence of Cerebral Aneurysms. Stroke 1997;28:799-804.
50. Bruno G, Todor R, Lewis I, Chyatte D. Vascular extracellular matrix remodeling in cerebral aneurysms. J Neurosurg 1998;89:431-40.
51. Stehbens WE. Etiology of intracranial berry aneurysms. J Neurosurg 1989;70:823-31.
52. Wei L, Wang Q, Zhang Y, Yang C, Guan H, Chen Y, Sun Z. Identification of key genes, transcription factors and microRNAs involved in intracranial aneurysm. Mol Med

 

Rep 2018;17:891-7.
53. Wáng YX, He J, Zhang L, Li Y, Zhao L, Liu H, Yang L, Zeng XJ, Yang J, Peng GM, Ahuja A, Yang ZH. A higher aneurysmal subarachnoid hemorrhage incidence in women prior to menopause: a retrospective analysis of 4,895 cases from eight hospitals in China. Quant Imaging Med Surg 2016;6:151-6.
54. Chalouhi N, Ali MS, Starke RM, Jabbour PM, Tjoumakaris SI, Gonzalez LF, Rosenwasser RH, Koch WJ, Dumont AS. Cigarette Smoke and Inflammation: Role in Cerebral Aneurysm Formation and Rupture. Mediators Inflamm 2012;2012:271582.
55. Jung KH. New Pathophysiological Considerations on Cerebral Aneurysms. Neurointervention 2018;13:73-83.
56. Wermer MJ, van der Schaaf IC, Velthuis BK, et al. Follow-up screening after subarachnoid haemorrhage: frequency and determinants of new aneurysms and enlargement of existing aneurysms. Brain 2005;128:2421-9.

**Cite this article as:** Roi DP, Mueller JD, Lobotesis K, McCague C, Memarian S, Khan F, Mankad K. Intracranial aneurysms: looking beyond size in neuroimaging: the role of anatomical factors and haemodynamics. Quant Imaging Med Surg 2019;9(4):537-545. doi: 10.21037/qims.2019.03.19

 